UNIVERSITY OF BIRMINGHAM

University of Birmingham Research at Birmingham

Spectro-temporal responses of curved railway tracks with variable radii of arc curves

Kaewunruen, Sakdirat; Ngamkhanong, Chayut; Liu, Xin

Document Version
Peer reviewed version

Spectro-temporal responses of curved railway tracks with variable radii of arc curves

Sakdirat Kaewunruen, Chayut Ngamkhanong

Department of Civil Engineering, School of Engineering, University of Birmingham, 52 Pritchads Road, Edgbaston B15 2TT, UK
s.kaewunruen@bham.ac.uk; cxn649@student.bham.ac.uk

Xin Liu

Department of Civil Engineering, Beijing Jiaotong University,
Haidian district, Beijing 100044, China
15125863@bjtu.edu.cn

On curved railway tracks, wheel/rail interface can usually cause a traveling source of sound and vibration, which constitutes high-pitch or tonal noise pollution causing a considerable concern of rail asset owners, commuters and people living or working along the railway corridor. The sound and vibration can be in various forms and spectra. The undesirable tonal sound on curves caused by excessive lateral wheel/rail dynamics resonance with falling friction states are often called 'squeal noises'. This paper evaluates the transient effect of curve radii on the possible occurrence of lateral track resonances, which is a principal cause of dynamic wheel/rail mode coupling that could trigger 'curve squeal'. This study is devoted to systems thinking approach and better insight into dynamic phenomena of railway tracks that could resolve the railway curve noise problems. Curved track models in three-dimensional space have been developed using a finite element package, STRAND7. The dynamic responses of curved track have been simulated by applying a moving train load. The transient loading model of a common wheel/rail slip has been adopted. The simulations of railway tracks with different curve radii have been carried out to develop state-of-the-art understanding into lateral track dynamics, including rail dynamics, dynamics, dynamics and overall track responses. Parametric studies have been conducted to evaluate lateral displacements, velocities and accelerations of rail over sleeper and rail at midspan both in static and dynamic conditions. The study firstly reveals that the lateral resonance of tangent tracks is relatively rare and the mode coupling behavior is unlikely to occur on moderately curved tracks. The lateral vibration responses have been presented in terms of time histories and spectro-temporal responses (also called "Spectogram"). The dynamic lateral responses of the track are found to be sensitive to the change of curve radii. The resonance peak in the lateral direction is related to the agreement of corresponding natural frequencies of rail and the vibration excitation frequencies under an individual rolling velocity. The outcome of this study establishes the new insight into the dominant influences of different track parameters to track lateral dynamic behaviors. Further studies will consider the effect of falling friction to cope the reality behavior.

Keywords: railway noise; system thinking approach; curve radius; lateral nonlinear dynamics; curve squeal; high-frequency vibration.

1. Introduction

Curve squeal is a strongly tonal noise emitted from wheel/rail contact caused by the passage of the train in tight curve rails with a low speed.[1, 2] The occurrence of squeal induces significant environmental impacts immensely annoying people living nearby due to its high frequencies characteristics.[3] Based on previous studies[4-7], unsteady lateral creepage of the wheel is thought to be the prime reason of squeal, while other mechanisms such as longitudinal creepage and flange contact, are determined to be of secondary importance reason of squeal noise but these seem to be a main source of flanging noise.[8-10] A number of research studies have been carried out to demonstrate the mechanism of squeal noise by means of site investigation and numerical modeling. Negative damping mechanism has been primarily proposed [10].The friction coefficient, which is relevant to the sliding velocity, falls after creepage exceeds the saturation point. This falling characteristic of creep force at high creepage is believed to be the main reason of squeal. However, the mode coupling instability as a new mechanism between normal and tangential dynamic is getting growing support while the negative friction mechanism is insufficient to explain some phenomena especially when the friction coefficient is almost constant .[1, 12] It is still questionable at which mechanism results in wheel/rail squeal.

Based on earlier studies, there are two main modeling approaches for curve squeal which are respectively in the time domain and frequency domain. The first approach introduces nonlinearities into the interaction model

while the computational efficiency as the calculation time is respectively high. Heckl and Abrahams,[13] investigated the vibration responses of an annular disc by applying a mathematical model which is excited by an oscillation force, acting at the disc circumference, normal to the plane of the disc. The modeling is performed in time domain rather than frequency domain allows the generation of curve squeal due to lateral creepage to be understood. Another paper[14] expanded the former model by presenting a frequency domain analysis of a friction-driven wheel according to the modal parameters of a wheel derived from the governing equation to assess which wheel will be prone to squeal. In order to figure out the frictional instability of wheel/rail contact, a detailed time domain model containing vertical and tangential wheel/rail interaction was contributed.[9, 15] The simulation demonstrated that squealing even appears in the case of constant friction not only just during the descent stage of friction based on a tangential contact algorithm TANG used to estimate the distribution of friction coefficients from the previous time step.

The variation of squeal noise have been observed on-site in conjunction with many critical parameters including curve radii, rail dynamics, cant dynamics and overall track response during operation. Previous work showed that squeal only occur when the curve radius is smaller than 100b, where b is the wheelbase of the bogie.[11] The results of on-site measurements also presented that there is no substantial reduction in wheel squeal associated with limiting operation speed. The investigation implemented by,[12] conducted the track dynamic in terms of fluctuation of curve noise after upgrading from timber sleepers to concrete sleepers. But the question remains as how other parameters change the lateral track dynamic. In fact, data collected in the field suggest a diverse range of curving behavior, which are largely relevant to curve radii.[16, 17] However, it is still uncertain to what extent the track lateral response is affected by rail radius. The occurrence of cant is believed to have positive impacts on reducing curve squeal due to its counteraction with creep force, an analytic approach has to be implemented for the determination of the effective range of cant. In reality, stable and unstable regimes of track deflection are predicted in operation condition due to high lateral load.[18] The track dynamic response characteristics need to be taken into account to justify the track dynamic under different lateral loads.

The critical review reveals the correlation between squealing and track vibration responses. However, lateral track dynamic characteristic has not been fully understood, especially when it comes to various curve radii, cants and lateral loads. It is noted that curve radii are the radii of circular arc. This study focuses on curved tracks with curve radii between 100m and 500m. This study aims to investigate the lateral track behavior into the effects of their properties. The present analyses are based on a detailed time-domain modeling, using Timoshenko beams in a general-purpose finite element package STRAND7 to build a two-dimensional track model that include the interaction between vertical and lateral directions. Both static and nonlinear transient analysis are carried out. Both vertical and lateral loads are applied to the railway track. Thus, the model covers the generation of squeal noise but does not include the sound radiation from the wheel due to the substitution of wheel by a pre-calculated impulse response function. Dynamic displacement, velocity and acceleration have been evaluated at rail over sleeper and rail at midspan under different curve radii and load cases. The lateral track vibration responses in frequency domain associated with squeal noise have been studied. Dynamic amplification phenomena are then highlighted. Based on previous studies, only a few papers focused on this area. The findings of this paper will provide some key parametric insights into fundamental dynamics of track in the lateral direction and establish the development of the dynamic design of curved track.

2. Numerical Method

2.1 Equation of track motion

The track model consists of a two-dimensional Timoshenko beam, which has been validated to be one of the most suitable options for concrete sleepers modeling due to its bending characteristic in the vertical and lateral directions.[19-20] To illustrate the nonlinearities of vibration of Timoshenko beam, the classical equations of motion are as follows:

$$\varepsilon = u_x + \frac{1}{2}w_x^2, \tag{1}$$

$$\kappa = \frac{\theta_x}{\sqrt{1+w_x^2}} \approx \theta_x(1 - \frac{1}{2}w_x^2 + \frac{3}{8}w_x^4), \tag{2}$$

$$\gamma = \tan^{-1}w_x - \theta \approx w_x - \frac{1}{3}w_x^3 - \theta, \tag{3}$$

where $u, w, \theta, \varepsilon, \kappa$ and γ represent the lateral displacement, the deflection, the cross-section rotation, the axial strain, the bending curvature, and the shear strain, respectively. The subscript x denotes the coordinate along the direction with the length of beam. The kinetic energy K and the strain energy U related to beam bending are given by

$$K = \frac{1}{2}\int_0^L \rho A w_t^2 dx + \frac{1}{2}\int_0^L \rho I \theta_t^2 dx, \tag{4}$$

$$U = \frac{1}{2}\int_0^L (EA\varepsilon^2 + EI\kappa^2 + kGA\gamma^2)dx, \tag{5}$$

where the subscript t represents partial differentiation with respect to time, ρ is the mass density per unit volume, A the area of the beam section, I the area moment of the inertia, E the Young's modulus, G the shear modulus and k the shear modification coefficient.[21]

2.2 Track Model

In this investigation, the finite element models of railway tracks have been previously developed and calibrated against the numerical and experimental modal parameters.[20-22] Fig. 1 presents the finite element models in three-dimensional space for an in situ railway track with both curve and tangent types. A commercial software STRAND7 is used for finite element simulation.[23] 2D Timoshenko beam has been chosen for track structure idealisation as a beam model since it has been found to be one of the most suitable options for modelling rail and concrete sleeper since its ability reflects the deep-beam-like structural behaviours.[24] This includes both shear and flexural deformations. Each sleeper consists of 60 beam elements and each rail consists of 200 beam elements. The overall model is represented by 1348 beam elements. The 60kg rail cross section were introduced in track model and the geometric parameters (Area: 17659.8mm²; Second moment of Area: 43.2x10⁶) were derived to be applied based on Australian Standard AS1085.1.[25] The trapezoidal cross-section was allocated to the sleeper elements with medium section (204mm top-wide250mm bottom-wide180mm deep). The rail pads under track were represented by a series of spring-dashpot elements. The distance offset between rail and sleepers was 100mm which does not have impacts on numerical results.[22-24] In the modeling, stiffness and damping values of high-density polyethylene pads were assigned to these spring-dashpot elements both in vertical and lateral direction. Ballast was placed under sleeper, supporting the rails and sleepers, which provide compression only. Tensionless beam support was used to achieve the support condition with allowance of hover over the support while the tensile supporting stiffness is omitted. In reality, tensionless support option can correctly reflect the real ballast characteristics.[25-31] Table 1 shows the geometrical and material properties of the finite element model. It was validated in previous studies, effects of length and boundary of track in this investigation (18 bays or 10.8m) on the computation and frequencies of interest are negligible.[19-20, 22]

Table 1. Engineering properties of rail

Length	$l_r =10.8$	m
Gauge	$g =1.5$	m
Modulus	$E_r =2.000e5$	MPa
Poisson's ratio	$v_r =0.25$	-
Density	$d_r =7850$	Kg/m³

Table 2. Engineering properties of rail pad

Vertical stiffness	$k_{pv} = 17$	MN/m
Lateral stiffness	$k_{pl} = 70$	MN/m

Table 3. Engineering properties of concrete sleeper

Length	$l_s = 2.5$	m
Spacing	$s = 0.6$	m
Modulus	$E_s = 3.75e4$	MPa
Shear modulus	$G_s = 1.09e4$	MPa
Density	$d_r = 2740$	Kg/m^3

Table 4. Engineering properties of ballast

|		
Ballast stiffness	$k_b = 13$	MN/m

In total, seven types of curve radii have been evaluated for dynamic investigations using curves ranging from
100m to 600m including a tangent one. Also, four types of cants are determined with the range from 0mm to
300mm. Engineering properties of each element are illustrated in Tables 1-4. These data have been validated by
a parametric analysis which is implemented in consideration of different rails, sleepers and ballast properties. In
order to adopt these, the partial support condition is believed to vastly conform with real condition of standard
gauge tracks. The nodes at both end of track were fixed in every direction to represent the track boundary. Both
ends of sleeper are constricted by hinge support to prevent lateral movement of sleeper. Four separated forces
with various magnitudes have been used to simulate the load condition of a passenger train bogie (2 per each
rail, 2 m apart). This load magnitude has been used for benchmarking purpose.[32-33] The schematic lateral load
case used is shown in Fig. 1c. The non-dimensional analyses were implemented to get the dynamic
amplification over curve radii and over frequency domain.
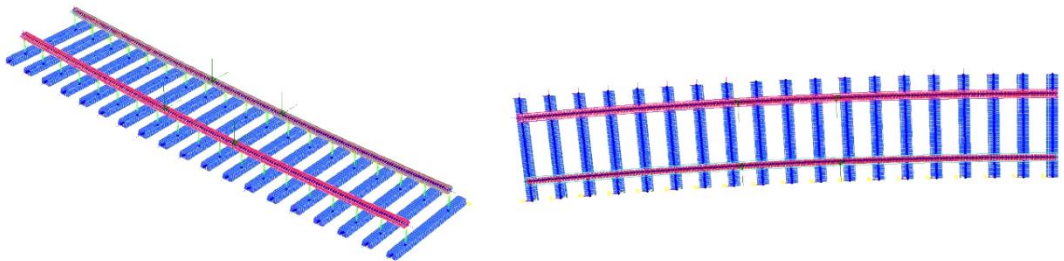
(a)
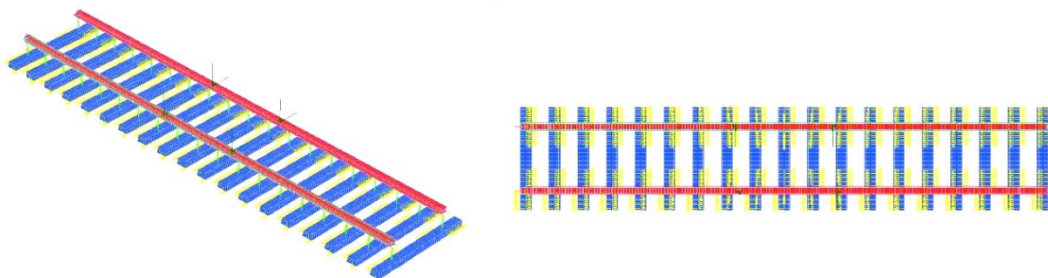
(b)
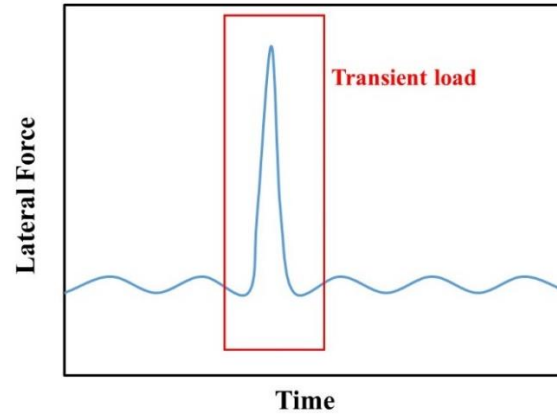
(c)

Fig. 1. Dynamic track models: (a) Model of curved track (b) Model of tangent track (c) Schematic load case

3. Results and discussions

The Linear Static Solver of STRAND7 has been used to evaluate the static response of railway tracks. For the static analysis, the position of lateral load coincides with the centroidal axis of rail model. The Nonlinear Transient Solver is then used to get dynamic behaviors of railway tracks after being verified by quasi-static condition. As indicated in Ref [34], noise is mainly developed by the wheel but not comes from the rail. The whole process of a passing train can be regarded as a series of moving loads and the track is supposed to be rigid for the entire analysis. Therefore, two moving load envelope with a speed of 10m/s have been established to evaluate the dynamic response of the rail based on an impulse excitation of a period of 0.0001s starting at time t =0.005s. The calculation time step is set to be 5×10^{-5} so that it can include high frequency modes for responses of curving. With this FE model, the eigenfrequencies and corresponding eigenmodes are calculated up to 10kHz, which is believed to cover modes of squeal noises vastly. The dynamic analyses are taken into account for various curve radii, cants and lateral loads. To appropriately take into consideration of dynamic effects of moving load, calculation time has been set to be 5s thus the entire process of dynamic responses can be adaptively reflected in simulation associated with the length of track and vehicle velocity. Lateral track displacements, dynamic acceleration have been evaluated both in static and moving load conditions. The output data obtained from simulation are more centering on dynamic responses at critical positions, including rail over sleeper and rail at midspan. The analysis positions are shown in Fig. 2. Dynamic factor can be computed as a ratio of dynamic response over static response. Typical deformation and stress distribution of a railway track under the lateral moving load are shown in Fig. 3. The rails present positive bending due to the lateral load applied perpendicular to load moving direction.
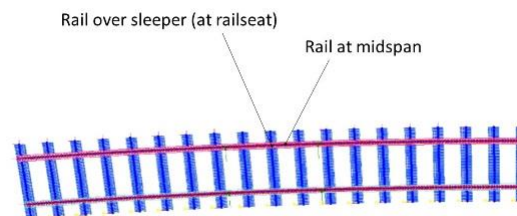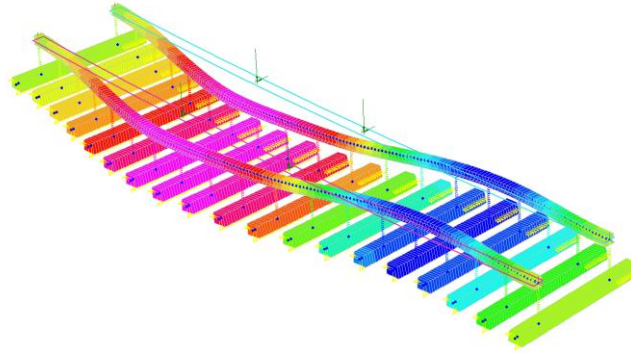

Fig. 2. Analysis positions

Fig. 3. Example of track's deformation under lateral moving load

3.1 Maximum displacement response

Fig. 4 illustrates a summary of maximum lateral dynamic displacements appearing on the track over sleeper with respect to different cants. The L/Vs are lateral to vertical load ratios where vertical load was selected as 100KN as a benchmark for passenger train bogie. Varying load ratios were comparatively investigated. Regarding the effects of curve radii, it is clear that the tracks with larger curve radii deform laterally more severe than tight curved tracks due to lower lateral resistance. The result can be effectively explained by arch mechanics that arches with larger curvature possess of higher compressive strength. The increase of track radius leads to a slower growth of rail lateral displacement which appears to be a general tendency for all the load cases. Therefore, the increase of lateral responses is nonlinear with respect to curve radius. It is exemplified by load ratio of 0.2, displacement increases 75.8% for curve radius varying from 100m to 200m, while the increase rate is only 3.2% for radius varying from 500m to 600m. This implies that lateral displacement responses are more sensitive corresponding to low radii, which gave evidence on the appearance of squeal during train negotiating tight curves. It can also be observed from the graph that the lateral track displacement of tangent track is similar to the value of track with a radius of 600m. For large curve radius, the lateral displacement of the track no longer change significantly with increasing radius therefore the increase of radius plays a little role on the dynamic amplitude of track. This phenomenon, in fact, is evident from the less flange contact between wheel and rail while train traveling in large curve. The results above indicate that the increased track radius may have positive effect on reducing curve squeal and squeal noise would disappear when the curve radius comes to a certain value.
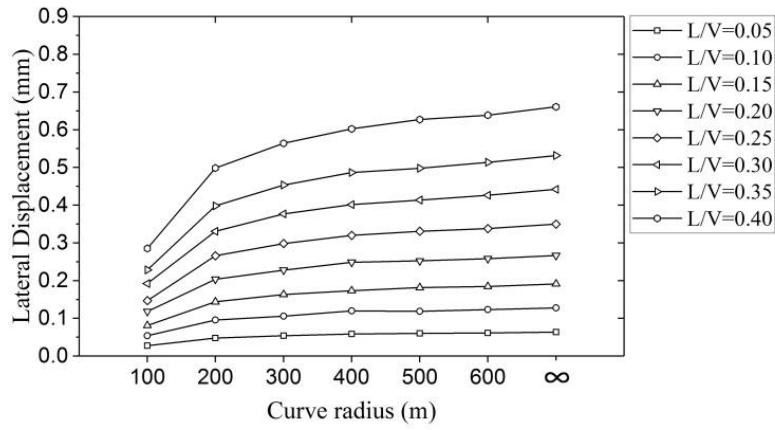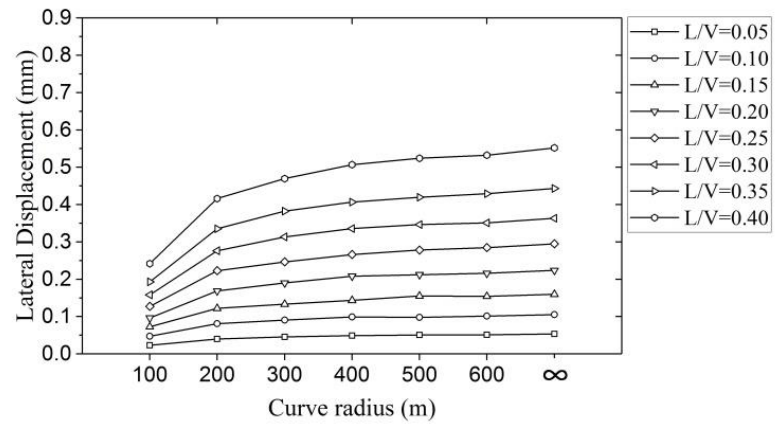

(a)

1
2 (b)

3
4 (c)

5
6 (d)
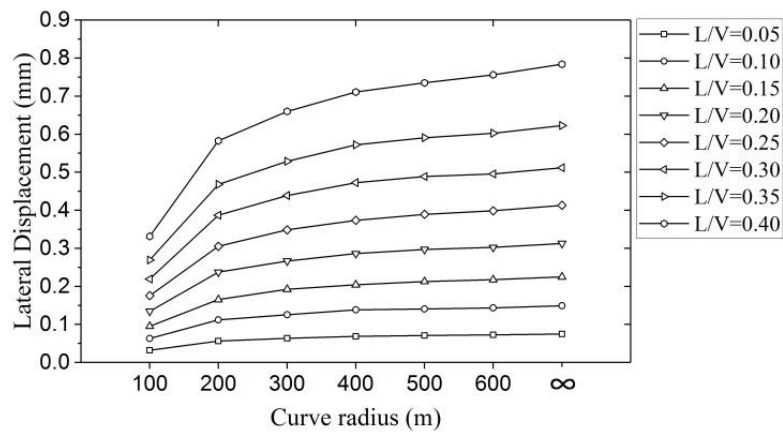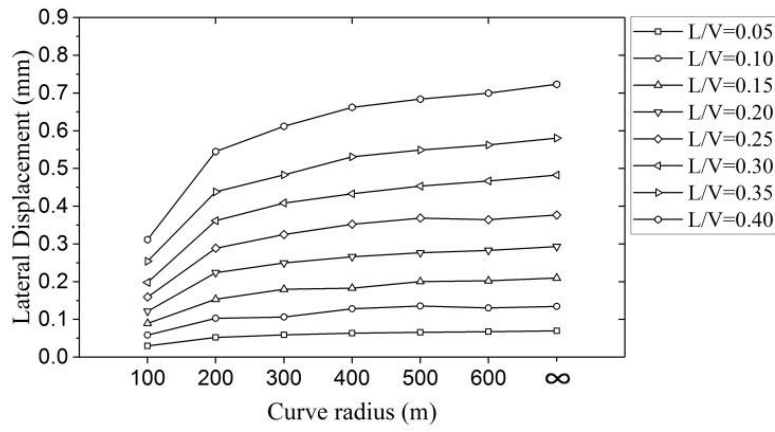
7 Fig. 4. Dynamic lateral displacements of track over sleeper at different curve radii under: (a) Cant = 0mm, (b) Cant = 100mm, (c) Cant =
8 200mm and (d) Cant = 300mm.

9 To evaluate the effects of cants on dynamic responses, Fig. 5 shows a comparison of dynamic lateral rail
10 displacements based on the simulation performed with a vehicle velocity of V=10m/s for varying cants. The
11 results apparently demonstrate the positive effect of including cant in curved track, which leads to a lower
12 dynamic response when cant goes towards a higher value. The result can be inferred by the occurrence of
13 centrifugal forces and compensative effect of cants. As expected, the railway track without a cant is more likely

1 to cause severe damage on track components and even leads to derailment. Therefore, these negative effects,
2 which could be avoided by adding suitable cants to railway track, should anyhow not obstruct railway normal
3 operation. The net axle lateral load is commonly assumed to be a key parameter that affects the simulation of
4 lateral dynamic responses.
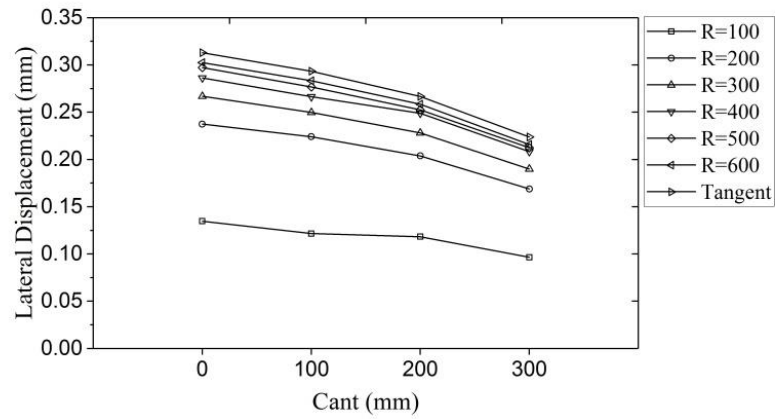
(a)
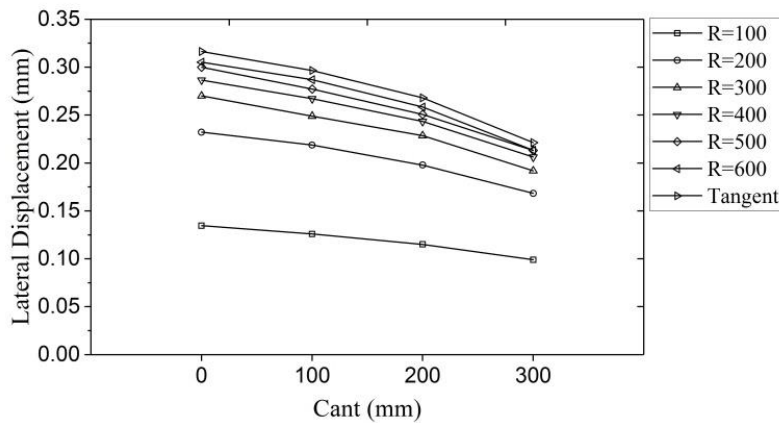
(b)

Fig. 5. Maximum lateral displacements of track at (a) Rail over sleeper and (b) Rail at midspan, with varying cants, L/V=0.2.

11 The load is typically to be represented as the ratio between the net axle lateral load to the axle vertical load
12 (L/V). Fig. 6 presents the results of the simulation in terms of a large range of lateral to vertical load ratios. Both
13 curved tracks and tangent track show almost identical results that an increase of L/V ratio gives rise to a rapid
14 growth rate of lateral rail displacement, causing further increase of displacement especially within a high load
15 range. Surprisingly, over L/V range of 0.05 to 0.2, no significant displacement fluctuation occurs while the
16 amplitude responses are generally to be unstable at load ratio above 0.2. For a curve of R=300m, the increase
17 rate of lateral displacement from ratio of 0.35 to 0.4 is 2.05 times than that of a low load ratio under the same
18 condition. The results suggest the nonlinearity of lateral responses, which is mainly due to the occurrence of
19 residual deflection under high lateral load. Based on previous studies, high lateral forces can cause distortion of
20 the track on the bed of ballast. For safety consideration, a limiting value of lateral to vertical load ratio should be
21 identified. The data in Fig. 6 illustrates that in case L/V ratio is under 0.35, the rail lateral displacements
22 stabilize at some finite value. Above this limit, the lateral displacement is found to increase at a rapid speed. The
23 results are consistent with the 85% Prudhomme formula. In addition, curved tracks are expected to exhibit more
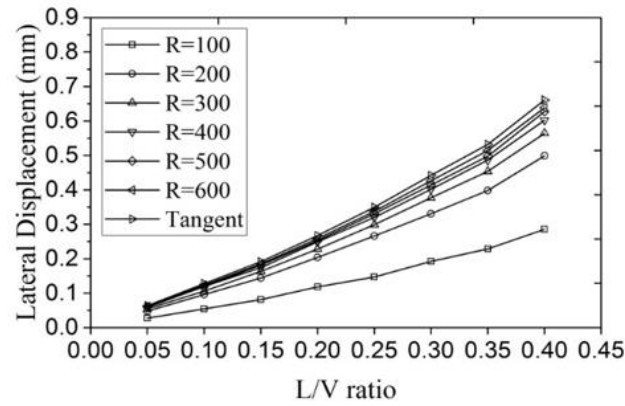24 severe unstable vibration than tangent track.

Fig. 6. Maximum lateral rail displacement under varying L/V ratio, cant=200m.
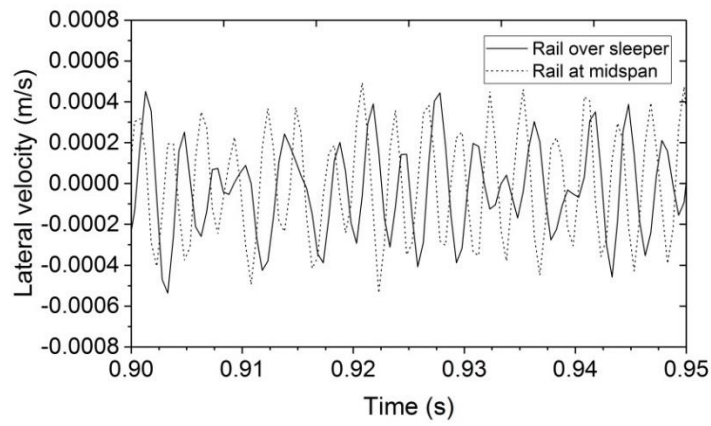
3.2 Lateral velocity

Fig. 7 shows the time histories of rail lateral velocity over sleeper (at railseat) and at midspan for the first 3 seconds in terms of a vehicle traveling at v=10m/s. The results are corresponding to a 20KN lateral load applied to the track with a curve radius of 100m. The lateral velocities at two positions appear to a similar varying pattern, the peak values of which are around 0.0006m/s. The graph for rail at mid-span is found to be fatter than that for rail over sleeper because of the bending behavior in Timoshenko beam at middle point. It can be demonstrated that the peak of the lateral velocity at rail does not occur at the position where train load is applied. There is a delay for the happening of maximum responses. The responses induced by the first sets of loads are smaller than that induced by following train load as a result of the superposition effects of moving loads. As the train load goes away, the velocities of track do not decrease immediately while a stabilization stage can be observed till the decay takes place at 2.0s. When zoomed in, it is found out that the over sleeper and midspan velocities changed from out of- phase to in-phase over approximately 50ms. The phase difference between these two positions reflects the bending characteristic when waves propagate along the track.
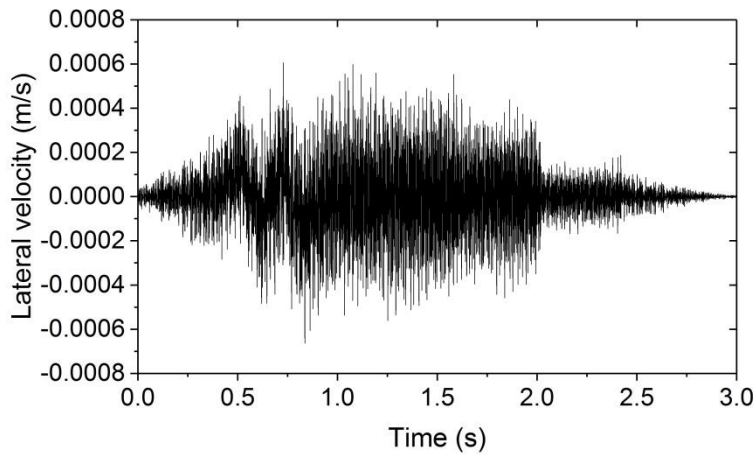

(a)
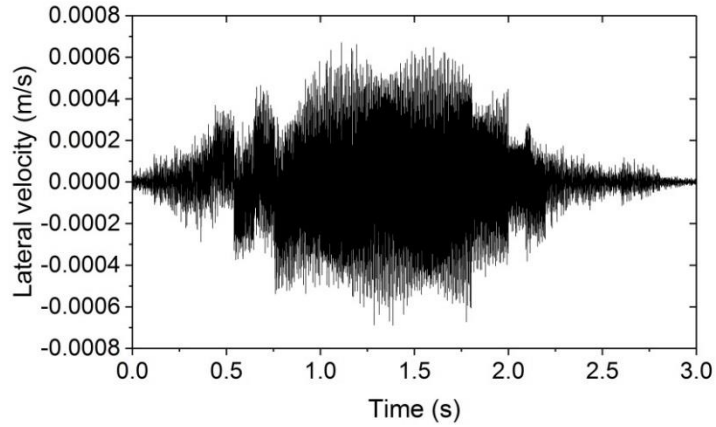
(b)

(c)

Fig. 7. Time history of track lateral velocity under radius of 100m, L/V=0.2: (a) Rail over sleeper, (b) Rail at midspan and (c) Comparison between rail over sleeper and rail at midspan.

The dynamic excitation feature is comprehensively exhibited in terms of the mobilities of the track. The lateral mobility spectrums obtained by a fast Fourier transform are shown in Fig. 8 as a comparison of three types of track by virtue of logarithmic distribution in dB re.10^{-9} m/s. The vibration levels in terms of dB are calculated by the ratio of one level respect with respect to a reference level ($20\log(V/V_{ref})$, $20\log(A/A_{ref})$) where V and A are velocity and acceleration, respectively. It should be noted that the decibel reference levels for velocity and acceleration (V_{ref} and A_{ref}) recommended by ISO R 1683 are 10^{-9} and 10^{-6}, respectively. Both for rail over sleeper and rail at mid-span, lateral mobilities in small radius perform higher values than that in large radius predominantly in the frequency between 1kHz and 5kHz which is of interest in generation of curve squeal. For responses of rail over sleeper, the resonance peak at 251Hz in lateral direction is related to natural frequency of both curve and tangent tracks. The lateral pinned-pinned anti-resonance and resonance appear at 370Hz and 730Hz respectively. Interestingly, the increasing of curve radius in both cases moves pinned-pinned resonance to higher frequencies and the depth of resonances are effectively reduced. For example, the sharp peaks at 730Hz significantly drop by 20dB with the transition of track radius from 200m to 500m. This is due to the fact that curve radius strongly affects track dynamics. However, below this frequency, the lateral mobilites are generally unaffected by the curve radius but in the frequency range 1000-5000Hz the responses from the various cases incur apparent differences due to the influence of wheel/rail interaction during the curving. When compared with curved track, tangent track globally exhibits much lower noise levels in high frequency, which implies curve squeal is not likely to occur under this condition. Moreover, modes above 5000Hz are mostly related to self-vibration. Therefore, curve radius has little effect on the track resonances in lower frequency range while has significant effect on reducing unstable eigenvalues in higher frequency range. As a

1 consequence, curve squeal can be effectively suppressed by increasing curve radius. The similar nonlinear
2 situation can be verified from track lateral responses at midspan.
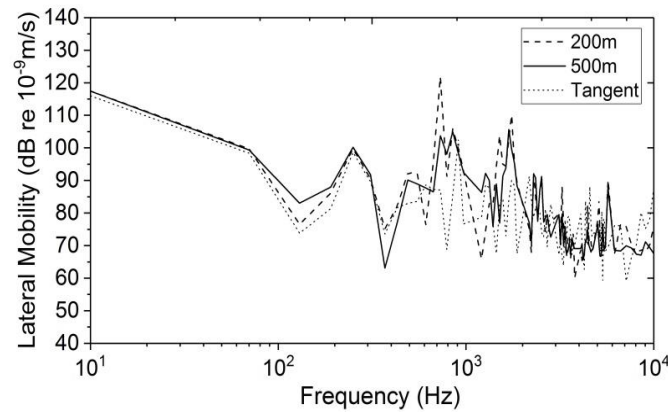
(a)
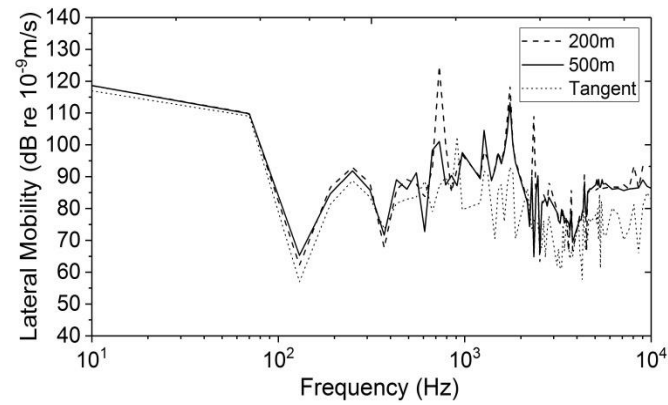
(b)

Fig. 8. Spectra of rail lateral mobility at (a) Rail over sleeper and (b) Rail at midspan for varying types of track.

8 The spectrograms of the track vibration velocity in the lateral direction during the train pass through the track
9 are shown in Fig. 9. The value of vibration velocities can be divided into three phases. The lowest range of track
10 velocity vibration can be observed within the low frequency range(less than 1000Hz). Between 1000Hz and
11 2000Hz, the values are higher than that within lower frequency and obviously separated from the range of more
12 than 2000Hz. A similar phenomenon can be observed in track with a radius of 500m while less unstable modes
13 appear in it. It can be concluded that when the track radius increase, the effect of lateral vibration velocity on
14 track decrease. In addition, track lateral vibration velocity increases due to the increase in frequency during the
15 passing train.
16
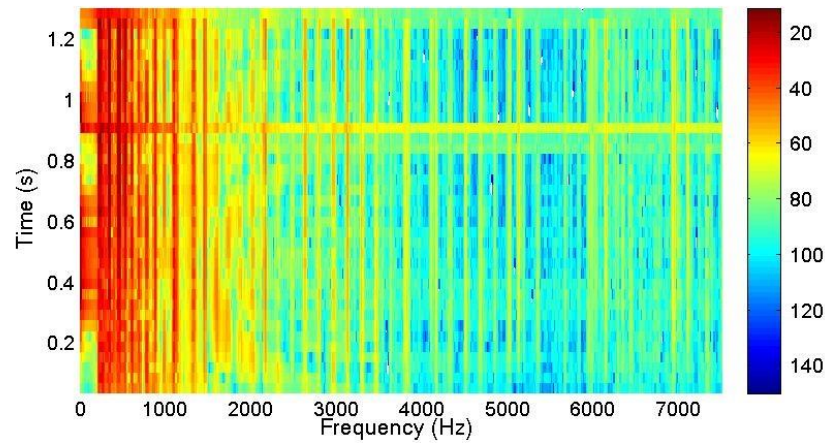
(a)
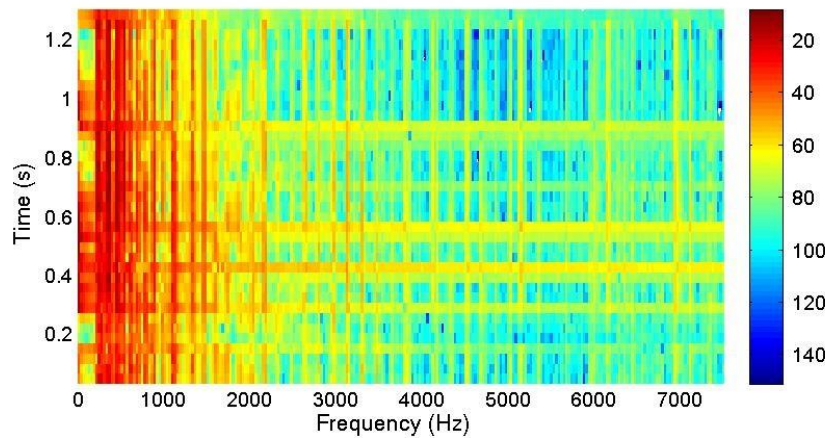
(b)

Fig. 9. Spectrogram of track lateral vibration velocity during train pass-by (a) R=200 (b) R=500.

3.3 Lateral acceleration

Rail vibration is now determined in Fig. 10 by giving the lateral point acceleration in time domain at rail joint over sleeper in terms of a 20KN lateral load applied to a curved track. In Fig. 10, the results measured at middle point of rail are also shown as a reference. These indicate that the responses in rail midspan are slightly higher at all period than those in rail over sleeper. This could be associated with the fact that the vibratory behavior of the track at midspan is similar to that of simply supported beam at the midpoint. It can be found that the peak responses for rail over sleeper and rail at midspan are $1.23 m/s^2$ and $1.54 m/s^2$ respectively. Note that both are positive acceleration values. The lateral acceleration of rail at midspan arrived at its peak till the train travels through the track and there is a stable fluctuation phase between around 1.0s and 2.0s. Note that the maximum lateral acceleration at rail over sleeper occurs before 1.0s as the moving loads reach the analysis position at rail over sleeper before midspan. The overall varying trend of acceleration is similar to that in time histories of velocity. The vibration responses of track are determined to abruptly vanish at 2 seconds, above which the variation of responses is relatively unimportant. Taking these results into consideration, it is judged that track responses differ significantly at varying positions.
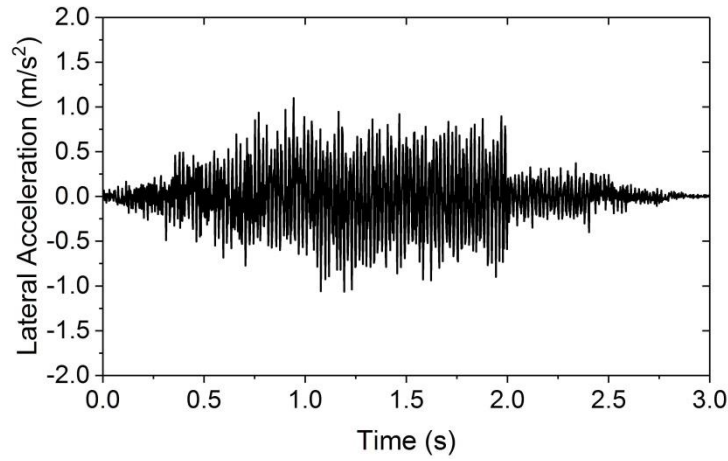
(a)
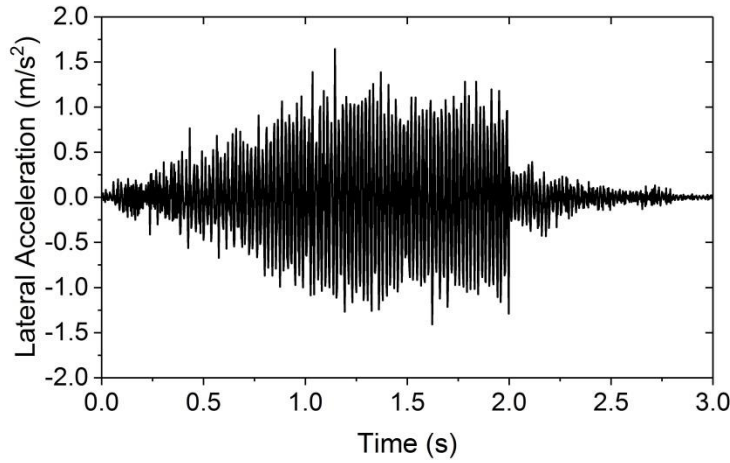
(b)

Fig. 10. Time history of track lateral acceleration under radius of 100m at (a) Rail over sleeper and (b) Rail at midspan.

Fig. 11 shows the corresponding Fourier spectrum for rail vibration at midspan with respect to curve radius of 200m, 500m and infinite. The most distinct resonance of 200m radius track occurs at 150Hz with the value of 131dB while the maximum response of 500m radius track happens at 251Hz with the value of 125.6dB. Therefore, the increase of track radius expands the resonance frequency and reduces the peak of vibration due to the time variation of response spectrum. It can also be verified by the fact that the acceleration in tangent track are lower than that in curved tracks. . On the contrary, the track acceleration in the frequency region of most interest for the squeal, 1000Hz-5000Hz, is much greater on 200m radius track than on 500m radius track and tangent track. This would lead to more unstable modes occur at squeal frequency region, which enhances the severity of squealing. When zoomed in, it can be found out that track with low radius is more susceptible to squeal noise as the receptances of the track with a radius of 200m enclose that of the track with high radius. A comparison of acceleration levels between curved track and tangent track suggests that vibration in tangent track in high frequencies tend to have less possibility of occurring of squeal noise.
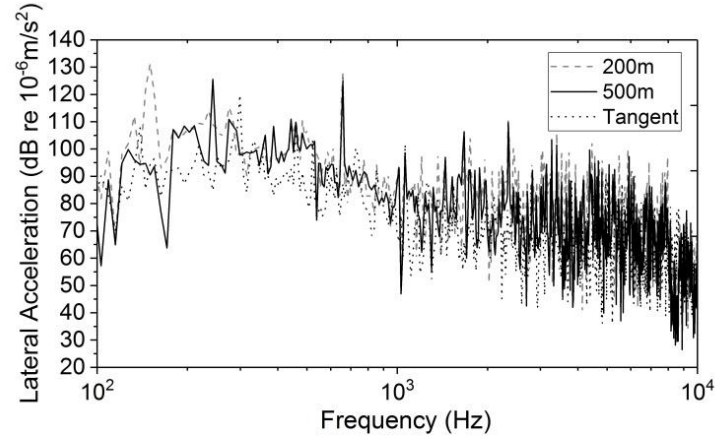
(a)
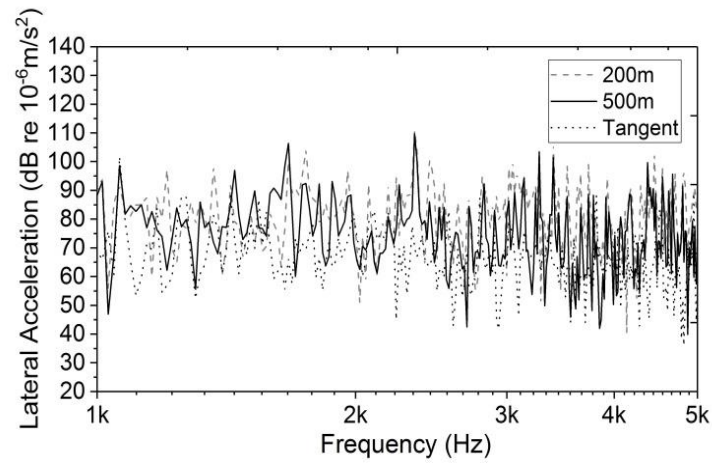
(b)

Fig. 11. Spectra of rail lateral acceleration at middle span of rail for varying types of track in frequencies range of

(a) 100-10000Hz and (b)1000-5000Hz

Fig. 12 illustrates the effect of curve radius by showing the difference between the responses of rail with radius of 200m and 500m. In order to show the reduction in track noises most clearly, insertion gain as an indication of vibration mitigation has been used here to quantify the relative mitigation effects. In overall frequency domain, the insertion gain distributes mainly in the range of -10dB-30dB. The region at frequencies below 1000Hz is much lower than that at frequencies between 1000Hz and 5000Hz where curve squeal is most likely to occur. Therefore, it is demonstrated that the responses of track in high frequencies are sensitive to track radius thus increasing of curve radius has significant positive effect on reducing squeal noise.
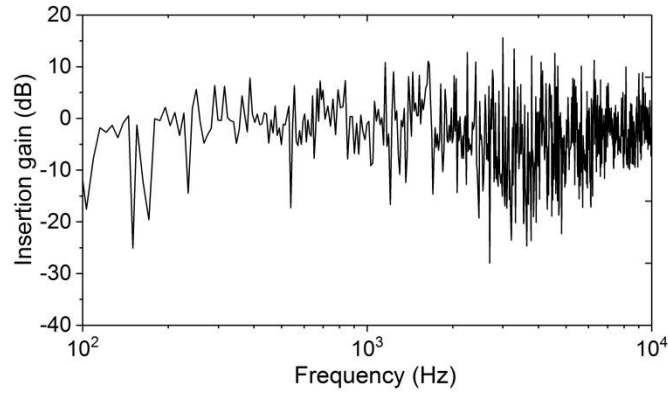
(a)
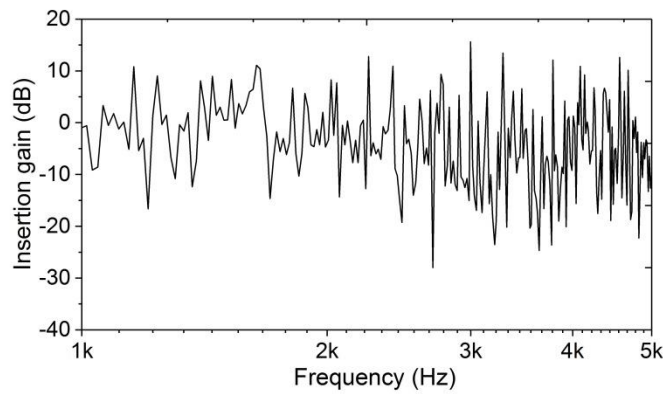
(b)

Fig. 12. Insertion gain of track responses with respect to change in track radius from 200m to 500m in frequencies range of

(a)100-10000Hz and (b) 1000-5000Hz.

3.4 Dynamic factors

In Fig. 13, the dynamic factors are investigated in terms of varying curve radii. Dynamic factors show discrete behaviors for varying curve radii due to unstable vibration modes excited by moving load. It clearly demonstrates that track without cant has poor performance in dampening rail vibration responses. On average, dynamic factor was reduced by more than 18% from cant of 0mm to cant of 100mm. This is due to the positive effect of centrifugal and gravitational balance. Therefore, higher cants can help to stabilize railway track by reducing dynamic responses of the rail over sleeper. In fact similar trend can be observed for rail at midspan. However, for cant of 300mm, surprising phenomenon occurs that dynamic factor is no longer to be reduced with the increase of cants. High cants lead to a more severe dampening performance of track. This is reverent to the dynamic characteristic of cants. It is clear that cant has a significant effect on track dynamic therefore the limiting value of which should be established to ensure the safety of railway operation.
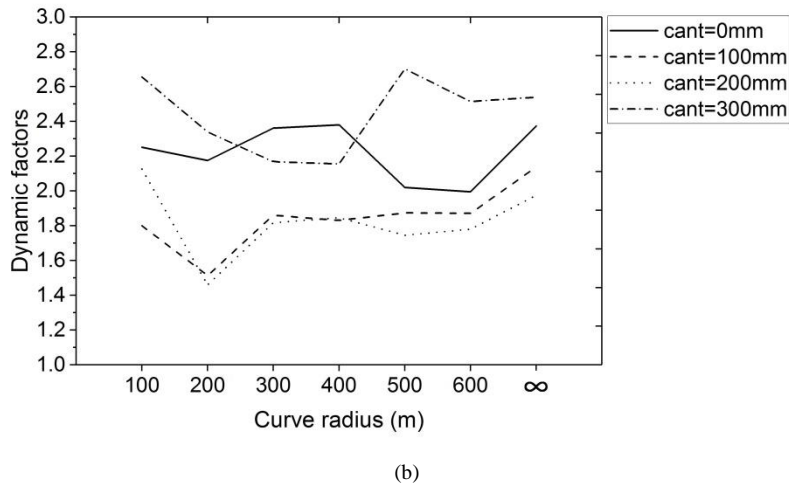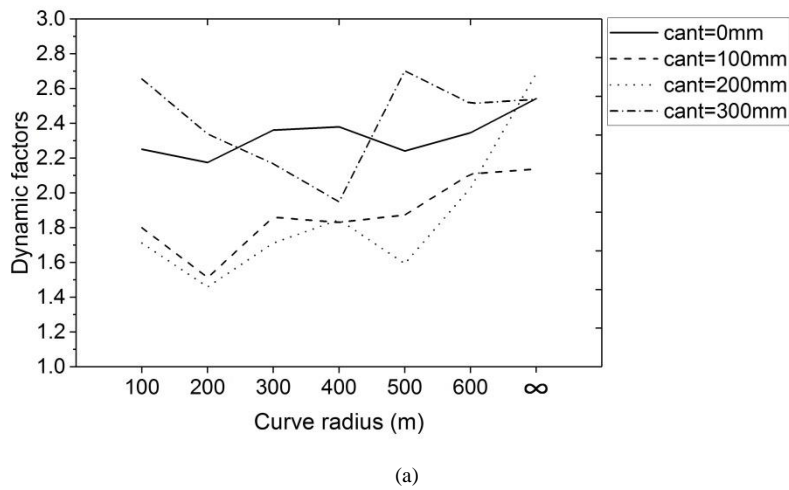
Fig. 13. Dynamic factors of track at (a) Rail over sleeper and (b) Rail at midspan, L/V=0.1.

4. Conclusion

In urban environment, curve squeal is an annoying problem due to its tonal nature and uncertain excitation mechanism. This type of noise is commonly emitted in tight curve rails. In this paper, a numerical simulation has been implemented to identify the lateral dynamic vibration characteristics of curved track with many influencing parameters including track radii, cants and lateral to vertical load ratios. The track model was established in three-dimensional space using a finite element package STRAND7. Parametric studies performed with curved track model have indicated many important results. The relative rail displacement can be reduced by the increasing of curve radius. However, for tight curve, relative displacement responses are more sensitive to the change of radius. This provides evidence on the occurrence of squeal in tight curve. Cant is believed to have positive effect on dynamic responses therefore adding cant is a valid approach to reduce the amplitude of track components. On the other hand, simulation captured instable tendency to dynamic responses for high lateral load where 0.35 can be used as a limitation of lateral to vertical load ratio. Spectro-temporal (also called "spectrogram") responses are presented in this study by representing the amplitude of lateral velocity vibration over time at various frequencies present in a particular waveform. In terms of lateral velocity, track responses differ apparently at varying positions. Mobilities of track show good consistency with respect to various tracks at low frequencies although resonances are generally moved to higher frequencies when a higher radius is applied. However, the resonance is not observed on tangent track. It is noted that increasing of track radius tends to vastly control the squeal noise at higher frequencies. Moreover, track acceleration in higher frequencies are more sensitive to the track radius. The insertion gain in squeal region is double of that in lower frequencies. In

comparison of results for different types of track it is determined that vibration in tangent track would not incur squeal noise since the resonance effect is not observed in the frequency range from 1000 to 5000Hz. Dynamic factor, as a significant parameter to reflect the track dynamic behaviors, is observed to fluctuate intensely with varying curve radii. Introduction of cants exhibits remarkable reduction of the dynamic amplification in comparison with absence of cants. However, a high cant is demonstrated to incur severe dampening performance therefore a reasonable range of cants need to be established. The study firstly exhibits that the lateral resonance of tangent tracks is not dominant and the mode coupling behavior may not occur on moderately curved tracks. This study establishes the new insight into the dominant influences of different track parameters to track lateral dynamic behaviors. However, further studies into dynamic and falling frictions are needed for investigations since the wheel/rail friction is not constant in reality. [35]

References
[1] D. Thompson, Chapter 9 – Curve Squeal Noise, *in: Railw. Noise Vib.*, (2009) 315–342.

[2] X. Liu, C. Ngamkhanong and S. Kaewunruen, Nonlinear dynamic of curved railway tracks in three-dimensional space. *3rd International Conference on Mechanical Engineering and Automation Science*, Birmingham, United Kingdom, 13-15 October 2017.

[3] A. Wickens, *Fundamentals of Rail Vehicle Dynamics: Guidance and Stability*, 2003.

[4] P.J. Remington, Wheel/rail squeal and impact noise: What do we know? What don't we know? Where do we go from here?, *J. Sound Vib.*, **116** (1987) 339-353.

[5] U. Fingberg, A model for wheel-rail squealing noise, *J. Sound Vib.*, **143** (1990) 365-377.

[6] D.J. Thompson and C.J.C. Jones, A review of the modelling of wheel–rail noise generation, *J. Sound Vib.*, **231** (2000) 519-536.

[7] F.G. de Beer, M.H.A. Janssens and P.P. Kooijman, Squeal noise of rail-bound vehicles influenced by lateral contact position, *J. Sound Vib., ***267** (2003) 497-507.

[8]   J.R. Koch, N. Vincent, H. Chollet and O. Chiello, Curve squeal of urban rolling stock-Part 2: Parametric study on a 1/4 scale test rig, *J. Sound Vib., ***293** (2006) 701–709.

[9] A. Pieringer, A numerical investigation of curve squeal in the case of constant wheel/rail friction, *J. Sound Vib.*, **333** (2014) 4295–4313.

[10] N. Vincent, J. Koch, H. Chollet and J. Guerder, Curve squeal of urban rolling stock - Part 1: State of the art and field measurements, *J. Sound Vib.* **293**(3) (2006) 691- 700.

[11] M.J. Rudd, Wheel/rail noise-Part II: Wheel squeal, *J. Sound Vib.*, **46**(3) (1976) 381–394.

[12] J. Jiang, I. Ying, D. Hanson and D.C. Anderson, An investigation of the influence of track dynamics on curve noise, *In: Noise and Vibration Mitigation for Rail Transportation Systems*, (2015) 441-448.

[13] M.A. Heckl and I.D. Abrahams, Curve squeal of train wheels, Part 1: Mathematical model for its generation, *J. Sound Vib.* **229**(3) (2000) 669–693.

[14] M.A. Heckl, Curve squeal of train wheels, Part 2: Which wheel modes are prone to squeal? *J. Sound Vib.*, **229**(3) (2000) 695-707.

[15] D. Anderson, N. Wheatley, B. Fogarty and J. Jiang, A. Howie, W. Potter W. Mitigation of Curve Squeal Noise in Queensland, New South Wales and South Australia, In: CORE 2008: Rail: The core of Integrated Transport, Perth, Australia, 7-10 September 2008, 7-10.

[16] S. Kaewunruen and A.M. Remennikov, Effect of a large asymmetrical wheel burden on flexural response and failure of railway concrete sleepers in track systems, *Eng. Fail. Anal.,* **15**(8) (2008) 1065–1075.

[17] S. Kaewunruen and A.M. Remennikov, Dynamic properties of railway track and its components: Recent findings and future research direction, *Insight Non-Destructive Test. Cond. Monit.*, **52**(1) (2010) 20–22.

[18] C. Ngamkhanong and S. Kaewunruen, B.J.A. Costa, State-of-the-art review of railway track resilience monitoring, *Infrastructures*, *3*(1) (2018).

[19] S.L. Grassie, Dynamic modelling of concrete railway sleepers, *J. Sound Vib.*, **187**(5) (1995) 799–813.

[20] S. Kaewunruen and A.M. Remennikov, Experimental simulation of the railway ballast by resilient materials and its verification by modal testing, *Exp. Tech.,* **32**(4) (2008) 29–35.

[21] M. Asghari, M.H. Kahrobaiyan and M.T. Ahmadian, A nonlinear Timoshenko beam formulation based on the modified couple stress theory, *Int. J. Eng. Sci.,* **48**(12) (2010) 1749–1761.

[22] S. Kaewunruen and A.M. Remennikov, Application of vibration measurements and finite model updating for structural health monitoring of ballasted rail sleepers with voids and pockets. *In: Mechanical Vibration*, Nova Science Publishers New York. (2009) 621-644.

[23] G+D Computing, Using Strand7: Introduction to the Strand7 finite element analysis system. Australia: Sydney, (2001).

[24] L. Falach, P. Paroni and P. Podio-Guidugli, A justification of the Timoshenko beam model through – convergence, *Analysis and Applications*, **15**(2) (2015) 261-277.

[25] Standards Australia, (2001) AS1085.1 Rail. Australia: Sydney, (2001).

[26] RailCorp, Engineering Specification SPC233 Concrete sleepers and bearers. Australia: Sydney, (2013).

[27] S. Kaewunruen and A.M. Remennikov, Effect of improper balalst packing/tamping on dynamic behaviors of on-track railway concrete sleeper, *International Journal of Structural Stability and Dynamics*, 7(1) (2007) 167-177.

[28] S. Kaewunruen and A.M. Remennikov, Effect of improper balalst packing/tamping on dynamic behaviors of on-track railway concrete sleeper, *International Journal of Structural Stability and Dynamics*, 8(3) (2008) 505-520.

[29] S. Kaewunruen, T. Lewandrowski and K. Chamniprasert, Effect of improper balalst packing/tamping on dynamic behaviors of on-track railway concrete sleeper, *International Journal of Structural Stability and Dynamics*, 18(1) (2018).

[30] C. Ngamkhanong, S. Kaewunruen and C. Baniotopoulos, A review on modelling and monitoring of railway ballast, *Structural monitoring and Maintenance*, 4(3) (2018) 195-220.

[31] Standards Australia, Australia Standard: AS1085.14-2003 Railway track material, Part 14: Prestressed concrete sleepers. Australia: Sydney, (2003).

[32] Kaewunruen S and Chamniprasart K (2016) Damage analysis of spot replacement sleepers interspersed in Chalmers University of Technology. In: Proceedings of the 29th Nordic Seminar on Computational Mechanics. Chalmers University of Technology Gothenburg, 28-30.

[33] O. Mirza, S. Kaewunruen and D. Galia, Seismic vulnerbility analysis of Bankstown's West Terrace railway bridge, *Struct. Eng. Mech.*, **57**(3) (2016) 569–585.

[34] R. Stefanelli, Curve squealing: Investigation of the general conditions which lead to squeal, and acoustic modeling of the squealing wheels. ETH Zurich, Issue ETH No.16686, 2006.

[35] S. Kaewunruen, Systems thinking approach for rail freight noise mitigation, *Acoust Aust,* 44: 193 (2016).

[36] S. Kaewunruen, J.M. Sussman and A. Matsumoto, Grand Challenges in Transportation and Transit Systems, *Frontiers in Built Environment*, **2**(4) (2016).